

RESEARCH ARTICLE

Rosiglitazone drives cavin-2/SDPR expression in adipocytes in a CEBP α -dependent manner

Björn Hansson[☯], Catarina Rippe[☯], Dorota Kotowska[☯], Sebastian Wasserstrom, Johanna Säll, Olga Göransson, Karl Swärd, Karin G. Stenkula*

Department of Experimental Medical Science, Lund University, Lund, Sweden

☯ These authors contributed equally to this work.

* karin.stenkula@med.lu.se



Abstract

Caveolae are abundant adipocyte surface domains involved in insulin signaling, membrane trafficking and lipid homeostasis. Transcriptional control mechanisms for caveolins and cavins, the building blocks of caveolae, are thus arguably important for adipocyte biology and studies in this area may give insight into insulin resistance and diabetes. Here we addressed the hypothesis that one of the less characterized caveolar components, cavin-2 (SDPR), is controlled by CCAAT/Enhancer Binding Protein (CEBP α) and Peroxisome Proliferator-Activated Receptor Gamma (PPARG). Using human mRNA expression data we found that SDPR correlated with PPARG in several tissues. This was also observed during differentiation of 3T3-L1 fibroblasts into adipocytes. Treatment of 3T3-L1-derived adipocytes with the PPAR γ -activator Rosiglitazone increased SDPR and CEBP α expression at both the mRNA and protein levels. Silencing of CEBP α antagonized these effects. Further, adenoviral expression of PPAR γ /CEBP α or Rosiglitazone-treatment increased SDPR expression in primary rat adipocytes. The myocardin family coactivator MKL1 was recently shown to regulate SDPR expression in human coronary artery smooth muscle cells. However, we found that actin depolymerization, known to inhibit MKL1 and MKL2, was without effect on SDPR mRNA levels in adipocytes, even though overexpression of MKL1 and MKL2 had the capacity to increase caveolins and cavins and to repress PPAR γ /CEBP α . Altogether, this work demonstrates that CEBP α expression and PPAR γ -activity promote SDPR transcription and further supports the emerging notion that PPAR γ /CEBP α and MKL1/MKL2 are antagonistic in adipocytes.

OPEN ACCESS

Citation: Hansson B, Rippe C, Kotowska D, Wasserstrom S, Säll J, Göransson O, et al. (2017) Rosiglitazone drives cavin-2/SDPR expression in adipocytes in a CEBP α -dependent manner. PLoS ONE 12(3): e0173412. doi:10.1371/journal.pone.0173412

Editor: Makoto Kanzaki, Tohoku University, JAPAN

Received: October 13, 2016

Accepted: February 10, 2017

Published: March 9, 2017

Copyright: © 2017 Hansson et al. This is an open access article distributed under the terms of the [Creative Commons Attribution License](https://creativecommons.org/licenses/by/4.0/), which permits unrestricted use, distribution, and reproduction in any medium, provided the original author and source are credited.

Data Availability Statement: All relevant data are within the paper submitted.

Funding: This work was financially supported by the Swedish Research Council (2013-3542 to K.St., K2015-65X-22662-01-3 to K.Sw.), The Novo Nordisk Foundation, Diabetes Foundation, Magnus Bergvall Foundation, The Crafoord Foundation, Albert Pahlsson Foundation, and the Royal Physiographic Society in Lund.

Competing interests: The authors have declared that no competing interests exist.

Introduction

Adipocytes constitute a major energy store and altered adipose tissue function is associated with development of obesity and diabetes. The plasma membrane of adipocytes is endowed with bulb-shaped invaginations called caveolae, enriched in cholesterol and sphingolipids [1]. These organelles are involved in insulin signaling, membrane trafficking and lipid homeostasis [2]. The integral membrane protein caveolin exists in three isoforms (CAV1-3), and is required for caveola formation [3]. In recent years, it has been demonstrated that the cavin proteins

(PTRF, SDPR, PRKCDBP, MURC) associate with the cytosolic side of caveolae and assist in their maturation [4, 5]. In humans, mutations in CAV1, CAV3 and PTRF cause lipo- and muscular dystrophies [6–8]. Moreover, genetic ablation of caveolae in mice causes impaired insulin receptor substrate (IRS)-1 signaling and insulin resistance [9–12]. Exploring the transcriptional regulation of caveolar components is therefore central for understanding adipocyte biology and may shed light on the link between caveolae and diabetes.

One of the less well studied cavins is cavin-2 (SDPR). This is a phosphatidylserine-binding protein [13] that was originally considered to target protein kinase C to caveolae [14]. In a landmark paper by Hansen et al. [15] it was found that cavin-2 knockdown led to a reduced abundance of caveolae at the surface of HeLa cells, whereas overexpression led to membrane tubulation. On the basis of these findings, cavin-2 was proposed to be critical for membrane bending in caveolae. Work on adipocytes, where cavin-2 is highly expressed [16], demonstrated that cavin-2 is an integral component of caveolae [16, 17]. Accordingly, cholesterol depletion led to degradation of cavin-2, redistribution of cavin-1 (PTRF), and loss of adipocyte caveolae [18]. Cavin-2 is also highly expressed in endothelial cells and *in vivo* knockout of cavin-2 reduces the density of caveolae in lung endothelial cells, but not in heart endothelial cells [19]. Cavin-2 therefore appears to be required for caveolae in adipocytes and lung endothelial cells, but possibly not for caveolae in other cell types. Such differential dependence on cavin-2 is likely dictated by the absolute expression levels, and by the cavin-2 to cavin-3 ratio, as the latter two cavins compete for binding to cavin-1 in a heterotrimeric complex [5]. Therefore, to understand how caveolae are generated in adipocytes and endothelial cells we must understand how cavin-2 expression is regulated.

Some recent inroads into the transcriptional control of cavin-2 have been made. Regazzetti et al. [20] demonstrated that hypoxia reduces cavin-2 expression via hypoxia inducible factors. Cavin-2 was also shown by us to be regulated by actin polymerization via the myocardin family coactivator MKL1 (MRTF-A) [21]. MKL1 is, to the best of our knowledge, the only positively acting transcriptional control mechanism for cavin-2 that has been described. Because recent studies have demonstrated that MKL1 counteracts adipogenesis, and because MKL1 is dramatically repressed in this process [22, 23], it is difficult to imagine that MKL1 could be responsible for the high expression of cavin-2 in adipocytes. Some other, positively acting, transcriptional control mechanism for cavin-2 is therefore sought to explain its high expression in adipose tissue [16].

Adipocyte formation, or adipogenesis, is a complex process involving many different transcription factors. The process can be modeled *in vitro* using e.g. 3T3-L1 cells exposed to adipogenic cues [24]. Two critical transcription factors are CEBP α (CEBPA) and PPAR γ (PPARG) [25]. These transcription factors induce each other's expression and jointly target key genes in adipogenesis [26]. Here we explored the possible role of CEBP α and PPAR γ for transcriptional regulation of cavin-2 in primary adipocytes. We demonstrate that PPAR γ and cavin-2 correlate in human tissues, that cavin-2 is upregulated during adipocyte differentiation in parallel with CEBP α and PPAR γ induction, and that CEBP α expression and PPAR γ -activation induces cavin-2 in primary adipocytes and their precursors. In all, these findings suggest that CEBP α /PPAR γ may represent an important transcriptional control mechanism for cavin-2/SDPR, and thus for caveolae, in adipocytes.

Materials and methods

Material

3T3-L1 cells were purchased from American Type Culture Collection. Quantifast SYBR Green RT-PCR kit (Qiagen, Holden, Germany), adenoviral vectors for GFP, MKL1, MKL2, CEBP α

and PPAR γ (GenBank accession number CU013410, BC171750, BC028890, and BC006811), were produced by Vector BioLabs Inc, (Philadelphia, USA). The PPRE-x3-TK-Luc reporter plasmid was a kind gift from Bruce Spiegelman (Addgene plasmid #1015) and SDPR reporter plasmid was obtained from Acive Motif (Nysdam, Belgium). Heat shock protein (HSP)90 and anti-caveolin-1 and -2 antibodies were from Cell Signaling Technologies (Danvers, USA). The anti-perilipin antibody was from Vala Science (San Diego, USA). Antibodies against PTRF (cavin-1) (ab48824) and SDPR (cavin-2) (AF5759) were from R&D Systems (Minneapolis, USA) whereas the PRKCDBP (cavin-3) antibody was from Proteintech (Rosemont, USA) (16250-1-AP).

Ethics statements

The Malmö/Lund experimental animal ethics Committee (Lund, Sweden) approved all procedures.

Preparation of primary adipose cells and adenoviral expression

Rat epididymal adipose cells were isolated from male Sprague Dawley rats, as described previously [27]. Cells were suspended in DMEM with Gentamicin (100 μ g/ml), phenyl-isopropyl-adenosin (PIA) (200 nM) and albumin (3.5% w/v), and cultured at 5% CO₂, 37°C for 20 hours with eGFP-MKL1, MKL2, CEBP α , PPAR γ 1 or control (GFP) virus. Virus treatment caused between 61 to 460-fold overexpression (S1 Fig, panel A). For MKL1, which had an eGFP tag, we confirmed overexpression by fluorescence imaging, showing that eGFP-MKL1 localized in the cytoplasmic rim, and prominently in the nucleus (S1 Fig, panel B).

RNA isolation

Cells and intact tissue were lysed and homogenized in Qiazol™ lysis reagent and RNA was isolated using RNeasy® Mini Kit (Qiagen) according to the manufacturer's recommendations.

RT-qPCR

PCR-reactions were performed using the Quantifast SYBR Green RT-PCR kit (Qiagen #204156) and Quantitect primer assays for 18S, MKL1, MKL2, CAV1, CAV2, PTRF, SDPR, PRKCDBP, PPAR γ 1, and CEBP α . Primer sequences are considered proprietary information by Qiagen. mRNA expression levels were measured using a StepOnePlus real-time thermal cycler (Applied Biosystems, Waltham, USA) and quantitated using the $\Delta\Delta C_T$ method as described by Livak and Schmittgen [28]. 18S mRNA expression levels were used for normalization throughout.

Transfection and luciferase assay

Isolated adipocytes were electroporated as described previously [29]. Briefly, isolated adipose cells were suspended (40% v/v) in DMEM supplemented with Gentamicin (100 μ g/ml) and PIA (200 nM) and electroporated (3 \times 12 ms, 500 V/cm) (Harvard Apparatus, Holliston, USA) with plasmids as indicated (reporter:promoter at 10:1). Afterwards, the cells were transferred into DMEM with Gentamicin, PIA, and BSA (3.5% w/v) and cultured for 20 h at 37°C in 5% CO₂. Cells were lysed in an equal amount of Promega passive lysis buffer and centrifuged at 1000xg for 10 min at 4°C. Luciferase activity was measured in a Glomax luminometer (Promega) using the Dual Luciferase Reporter (Promega) (PPRE) or LightSwitch Luciferase (ActiveMotif) (SDPR) systems.

Cell culture and CEBPA silencing

3T3-L1 fibroblasts were cultured and differentiated as previously described [30]. In short, cells were cultured at sub-confluence in DMEM medium containing 10% FCS (v/v) and 1% penicillin/streptomycin (v/v) in an atmosphere with 5% CO₂ at 37°C. For differentiation, cells were incubated with DMEM medium containing 10% FCS (v/v), 1% penicillin/ streptomycin (v/v), 0.5 mM 3-isobutyl-1-methylxanthine (IBMX), 10 µg/ml insulin and 1 µM dexamethasone for 48 h two days post confluence (designated day 0). Medium was changed to DMEM with 10 µg/ml insulin for 48 h and thereafter cells were cultured in DMEM containing 10% FCS (v/v) and 1% penicillin/ streptomycin (v/v) until day 9. In a subset of experiments, 3T3-L1 cells were treated with Rosiglitazone (1 µM, Sigma) for the time indicated in the figures. CEBPA silencing was performed as previously described [31] by electroporation at day 4, using siRNA targeting CEBPA (Ambion, ID: 63853 and 63854) or scrambled (Scr) siRNA (Ambion, Neg control #1 siRNA). After 24 hours, cells were stimulated for 20 hours with Rosiglitazone before collecting RNA and protein as described above.

Oil Red O staining

3T3-L1 cells (day -2 and 9) were washed in PBS, fixed with 4% formaldehyde for 1h and washed twice with water. Cells were incubated with Oil Red O (Sigma) solution (8.57mM Oil Red O in isopropanol) mixed 6:4 with water for 1 h and washed twice in water. Representative images were captured using an Olympus 1X71 system (Center Valley, USA), 10x objective NA 0.25.

Confocal imaging

Preparation of cells for microscopy was done as previously described [30]. Briefly, isolated primary adipocytes were washed twice in Krebs-Ringer (KRH) buffer containing 25 mM Hepes pH 7.4, 200 nM adenosine, 2 mM glucose, followed by fixation in 4% paraformaldehyde (PFA) for 6 min, and then washed twice in PBS pH 7.4, followed by blocking and permeabilization in KRH buffer with 0.1% Saponin for 30 min. To visualize polymerized actin, fixed cells were incubated with fluorescent conjugated Phalloidin-647 (Molecular Probes, Thermo Fisher Scientific, Waltham, USA) at a concentration of 165 nM for 20 minutes at room temperature. Cells were washed twice in PBS and imaged using a Nikon A1 plus confocal microscope with a 60x Apo DIC oil immersion objective, NA 1.40 (Nikon Instruments Inc.). Phalloidin-647 was excited at 640 nm and emission detected between 663–738 nm. All images were identically subjected to background subtraction and threshold settings. Images were acquired with NIS-elements, version: 4.50.02, (Laboratory Imaging).

Western blotting

Western blotting was performed as described previously [30]. In short, following incubations, cells were washed with KRH medium without BSA and subsequently lysed in a buffer containing 50 mM Tris/HCl pH 7.5, 1 mM EGTA, 1 mM EDTA, 0.27 M sucrose, 1% NP-40, and complete protease-and phosphatase inhibitor cocktail (Roche, Basel, Switzerland) (one tablet each/ 10 ml buffer). Lysates were centrifuged for 10 min at 13000xg and protein concentrations were determined using the Bradford method. Samples were subjected to polyacrylamide gel electrophoresis and electro-transfer to nitrocellulose membranes. Membranes were blocked and probed with the indicated antibodies. Detection was performed using horseradish peroxidase conjugated secondary antibodies and enhanced chemiluminescence reagent. The signal was visualized using a BioRad Image camera (Biorad, Hercules, USA).

Results

PPAR γ expression correlates with expression of cavin-2/SDPR in human tissues

We approached the question of transcriptional control mechanisms for cavin-2 (SDPR) using mRNA expression data obtained from the Genotype-Tissue Expression (GTEx) portal [32]. Correlations at the mRNA levels for SDPR versus PPAR γ (PPARG) and for SDPR versus CEBP α (CEBPA) were examined using Spearman statistics. Significant positive correlations between PPARG and SDPR were observed in human subcutaneous adipose tissue, in tibial artery, and in skeletal muscle (Fig 1A–1C). For CEBPA, on the other hand, no correlation was seen in adipose tissue, whereas a strong positive correlation was present in the tibial artery, and a weak negative correlation was observed in skeletal muscle (Fig 1D–1F). We also found a positive correlation between CEBPG and SDPR in adipose tissue ($P < 0.0001$, $R = 0.21$, not shown). These findings suggested the possibility that PPAR γ may contribute to the transcriptional control of SDPR. Among the five human tissues with the highest SDPR expression (TMM normalized reads), at least two, possibly three including breast, are dominated by adipocytes (Fig 1G). We therefore henceforth focused on regulation of SDPR in adipocytes and their precursors.

PPARG and CEBPA correlate with cavin-2 expression during adipocyte differentiation

Differentiation of 3T3-L1 cells into adipocytes in culture was initiated by adding an adipogenic cocktail. Conversion into adipocytes was examined using Oil-Red O staining, confirming that a majority (80%) of the cells acquired lipid droplets 9 days after commencement of differentiation compared with non-differentiated (-2 days) cells (Fig 2A). mRNA was extracted at day -2, 2, 4 and 9 for qPCR analyses. The expression of PPARG and CEBPA increased gradually during differentiation as expected (Fig 2B). Both PPARG and CEBPA were found to correlate with the expression of SDPR, and, in accordance with our findings in human adipose tissue, correlation with PPARG was tighter (Fig 2C, left vs. right). The expression of SDPR mRNA increased exponentially and in parallel with the protein during differentiation (Fig 2D). Other caveolae proteins along with perilipin, a definitive adipocyte marker, increased as well (Fig 2E).

3T3-L1 cells were next treated with the PPAR γ activator rosiglitazone (Rosi, 1 μ M) during differentiation (from day 4 through day 9). As predicted from the correlation analyses, Rosiglitazone significantly increased the expression of SDPR (Fig 2F). A small effect was seen on cavin-1 (PTRF), but levels of caveolin-1 (CAV1) and cavin-3 (PRKCDBP) were unaffected (Fig 2F). Our findings so far therefore suggested that cavin-2 may be regulated by PPAR γ /CEBP α during adipocyte differentiation.

Overexpression of CEBP α and PPAR γ activation increase SDPR expression in primary adipocytes

We next used adenoviral overexpression to examine if CEBP α and PPAR γ can drive expression of cavin-2 in primary white adipocytes from rat. Overexpression of CEBP α caused a 3–4-fold increase of SDPR expression, whereas other cavins and caveolins analyzed were unaffected (Fig 3A). PPAR γ and the myocardin family coactivators MKL1 and MKL2 were similarly unchanged (Fig 3A). Overexpression of PPAR γ induced expression of SDPR (Fig 3B), albeit with borderline significance ($p = 0.0503$ using a two-sided t-test, $p = 0.02$ using a one-sided t-test). Since PPAR γ is a ligand-activated receptor, we also treated primary adipocytes

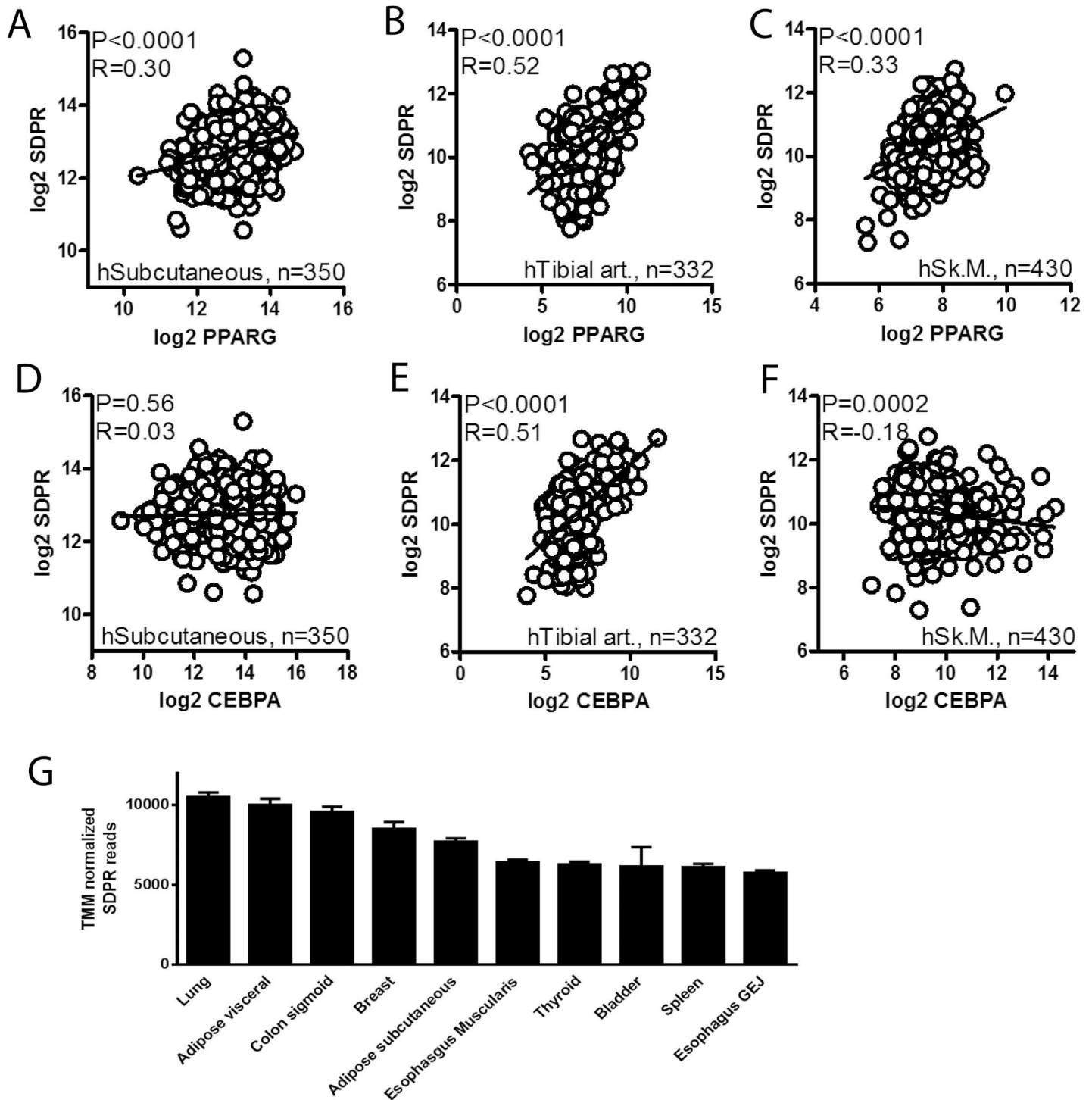


Fig 1. PPAR γ expression correlates with cavin-2/SDPR expression in human tissues. Panels A through F show correlations between PPARG and SDPR and between CEBPA and SDPR mRNA levels in the indicated human tissues. RNA-Seq data is from the Genotype-Tissue Expression (GTEx) portal [32] and normalization was according to the trimmed mean of M-values method. Correlations were tested using the Spearman method in GraphPad Prism 5. Nominal P-values (P) and Spearman's rank correlation coefficients (R) are given in the panels. Panel G shows TMM normalized RNA-Seq reads (means \pm SEM) for SDPR in the top ten expressing tissues in the database.

doi:10.1371/journal.pone.0173412.g001

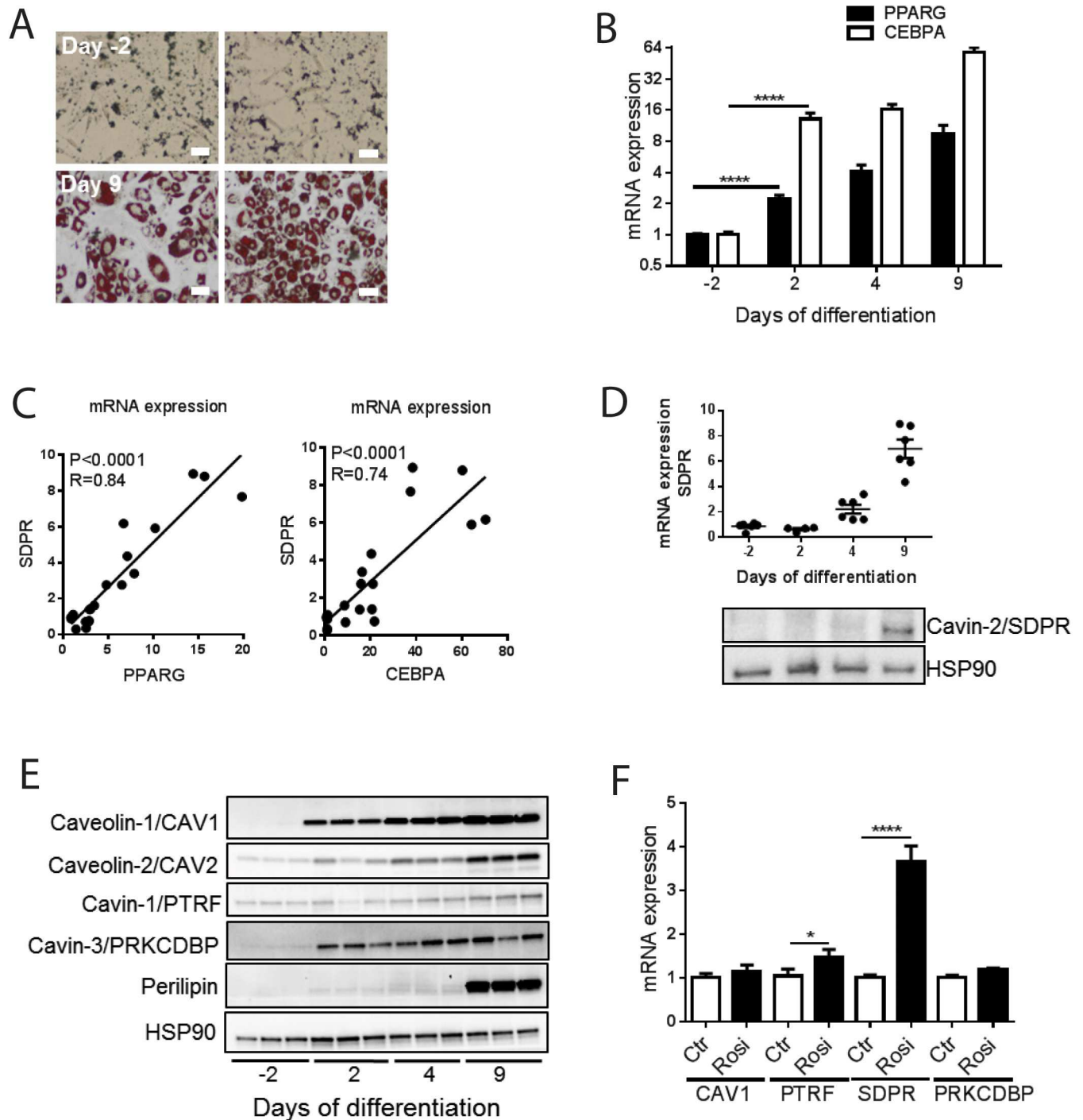


Fig 2. PPARG, CEBPA and SDPR expression during adipocyte differentiation of 3T3-L1 cells and the effect of the PPAR γ activation using rosiglitazone. 3T3-L1 cells were treated with adipogenic cocktail on day 0 and allowed to differentiate into adipocytes for 9 days. Panel A shows two representative light microscopy images of 3T3-L1 cells incubated with Oil-Red O prior to differentiation (day -2), and following 9 days of differentiation. Bar = 10 μ m. Panel B shows mRNA expression for PPARG and CEBPA, measured by qPCR at different time points of differentiation (-2, 2, 4 and 9 days). Panel C shows correlations between PPARG and SDPR and between CEBPA and SDPR, respectively, during adipocyte differentiation. Panel D shows mRNA expression and western blots for SDPR, and panel E western blots for caveolins and cavin-1 and -3 at different time points of differentiation. Cell lysates were collected and subjected to western blotting to detect total protein levels caveolin-1 (CAV1), caveolin-2 (CAV2), cavin-1 (PTRF), cavin-3 (PRKCDBP) and perilipin. HSP90 was used as loading control. Representative blots from $n = 3$ independent experiments with each sample run in triplicates are shown. Panel F shows the effect of treatment with the PPAR γ activator rosiglitazone (1 μ M, from day 4 to day 9) on the mRNA levels of caveolins and cavin-1/3. DMSO was used as vehicle control. Data in (B and F) is presented as means \pm SEM, * $p \leq 0.05$, ** $p \leq 0.01$, and **** $p \leq 0.0001$.

doi:10.1371/journal.pone.0173412.g002

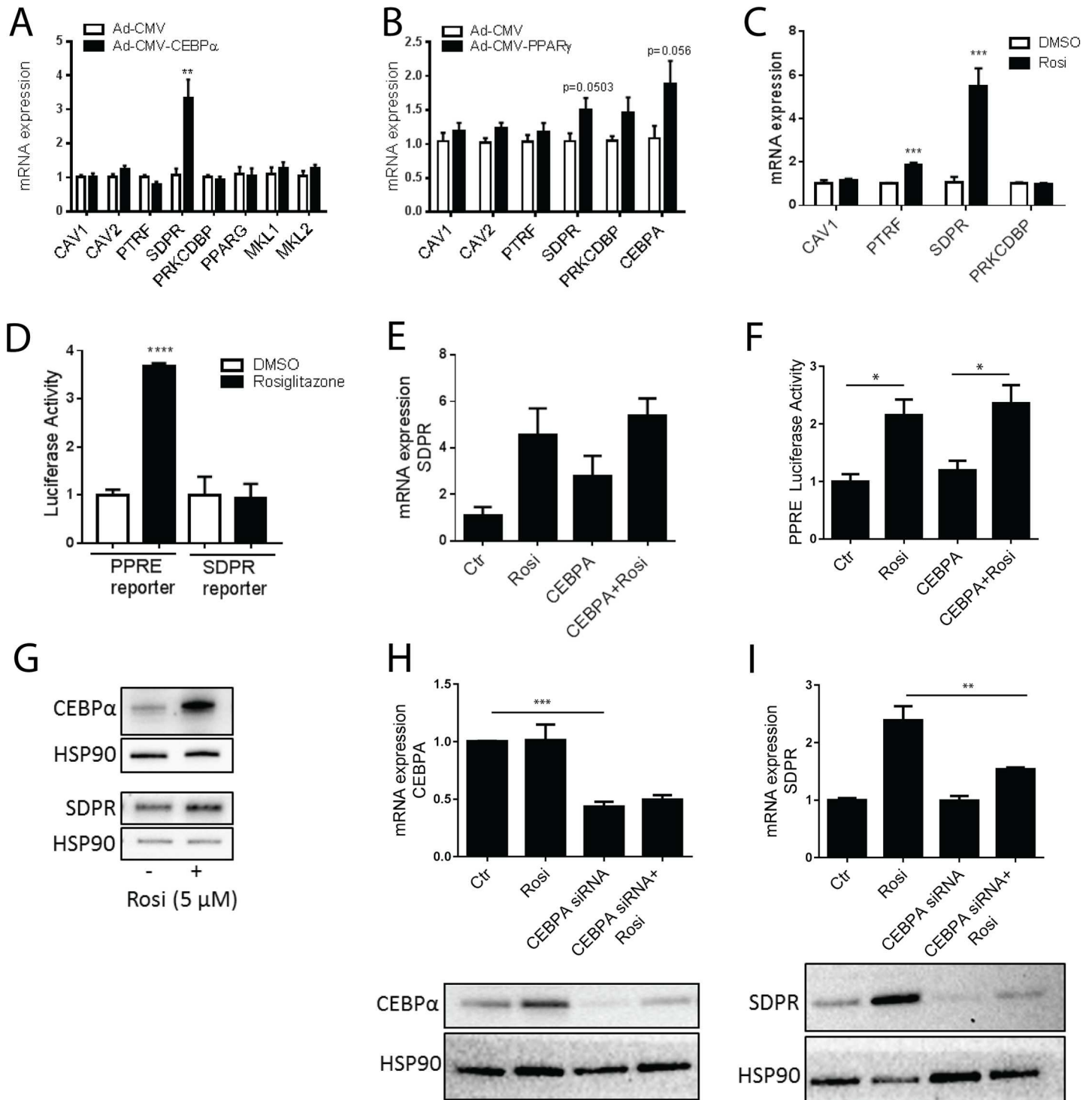


Fig 3. Overexpression of CEBPα and PPARγ activation increase SDPR expression in primary adipocytes. Panels A and B show qPCR analysis of caveolin and cavin expression in primary rat adipocytes following 20–24 h of incubation with adenovirus encoding CEBPα (Ad-CMV-CEBPα) (A), PPARγ (Ad-CMV-PPARγ) (B) or control adenovirus (Ad-CMV-null). n = 6 independent experiments. Adipocytes were incubated with Rosiglitazone (5 μM) or vehicle (DMSO) for 20–24 h, and the relative expression of CAV1, CAV2, PTRF, SDPR, and PRKCDBP analyzed using qPCR (C, n = 4 independent experiments). In panel D (left bars), adipocytes were transfected with PPRE luciferase reporter and Renilla reporter plasmids, followed by overnight (20 h) incubation with Rosiglitazone (5 μM) or vehicle (DMSO). Luciferase activity was measured in cell lysates using a luminometer, and the values normalized to Renilla luciferase activity. Each sample was measured in triplicate (n = 3 independent experiments). Adipocytes were also transfected with an SDPR promoter reporter (right bars) and incubated overnight (20 h) with Rosiglitazone (5 μM) or vehicle (DMSO). Cell lysates were subjected to luciferase activity assay and

each sample was measured in triplicate. $n = 3$ independent experiments. Adipocytes were incubated with DMSO (ctr), CEBP α adenovirus, Rosiglitazone (5 μ M), or their combination overnight (20 h), and analyzed using qPCR (E, $n = 3$ independent experiments). In panel F, adipocytes were transfected with PPRE luciferase reporter and Renilla reporter plasmids, followed by overnight (20 h) incubation with adenovirus encoding CEBP α , Rosiglitazone (5 μ M) or vehicle (DMSO) as indicated. Cell lysates were subjected to luciferase activity assay and each sample was measured in duplicate. $n = 3$ independent experiments. Western blot showing CEBP α and SDPR in cell lysates from primary adipocytes incubated with or without Rosiglitazone 20 h (DMSO, ctr). HSP90 was used as loading control. (G). In H, CEBPA was silenced using siRNA (or scrambled (ctr)) in 3T3-L1 cells on day 4 of differentiation. At day 6, cells were stimulated with Rosiglitazone (1 μ M) for 20 h. $n = 3$ independent experiments, each sample run in duplicate. CEBP α silencing was confirmed by western blotting, representative image is shown below graph (H). mRNA expression of SDPR following CEBPA silencing is shown in I. Protein level of SDPR shown below graph (I). HSP90 used as loading control (H and I). Data is presented as means \pm SEM, * $p < 0.05$, ** $p < 0.01$, *** $p < 0.001$, and **** $p < 0.0001$.

doi:10.1371/journal.pone.0173412.g003

with rosiglitazone (5 μ M, 20 h). qPCR analysis demonstrated a marked, 5–6-fold, induction of SDPR in Rosiglitazone-treated adipocytes (Fig 3C). PTRF also increased, but the expression of CAV1 and PRKCDBP was unaffected (Fig 3C).

PPAR γ activity and SDPR promoter activation were next examined using luciferase reporter assays. These assays showed that Rosiglitazone caused a 3-fold increase in PPAR γ activity compared with DMSO-treated control cells (Fig 3D), providing a positive control for the treatment. The proximal SDPR promoter (\approx 1000 nt) was however not activated by Rosiglitazone from the same batch and at the same concentration (Fig 3D), suggesting involvement of a distal enhancer.

We also examined if CEBP α and PPAR γ were acting synergistically. Somewhat to our surprise, the effects of Rosiglitazone and CEBP α appeared to be non-additive (Fig 3E). The PPAR response element (PPRE) reporter was not responsive to CEBP α expression, ruling out that CEBP α works through PPRE (Fig 3F), but leaving the possibility that Rosiglitazone acts indirectly on SDPR through PPAR γ -mediated induction of CEBP α . This hypothesis was supported by the observation that overnight incubation with Rosiglitazone increased the protein levels of CEBP α and SDPR (Fig 3G). Silencing of CEBPA in 3T3-L1 cells (Fig 3H) significantly suppressed the Rosiglitazone-driven SDPR expression (Fig 3I), without altering the non-stimulated SDPR level (Fig 3I, Ctr versus CEBPA siRNA). Western blotting confirmed that Rosiglitazone increases both CEBP α (Fig 3H, lower panel) and cavin-2 (Fig 3I, lower panel) expression in 3T3-L1 cells, and that CEBPA silencing diminished this effect (Fig 3H and 3I, lower panels). These findings show that CEBP α and PPAR γ , key lineage specifiers in adipocytes, have the ability to drive expression of SDPR in both mature adipocytes and their precursors and that the level of CEBP α , indirectly controlled by PPAR γ , exerts a transcriptional drive on cavin-2.

MKL1 and MKL2 drive expression of caveolins and cavins but SDPR expression is unresponsive to actin depolymerization in primary adipocytes

In recent work it was found that myocardin family coactivators (MYOCD and MKL1) are able to regulate the expression of all caveolins and cavins in smooth muscle cells [21]. MKL1, which is highly expressed in mesenchymal cells, downregulates PPAR γ and is repressed during early stages of adipogenesis [23]. This is critical for normal adipocyte maturation. In human adipose tissue, we found that MKL2 reads [32] were ten-fold higher than those of MKL1 (not shown). We therefore next explored the possible effects of both MKL1 and MKL2 on caveolin and cavin expression in adipocytes. By qPCR analysis, we found that viral overexpression of MKL1 and MKL2 increased the expression of essentially all caveolins and cavins in primary rat adipocytes and moreover repressed CEBP α and PPAR γ (Fig 4A and 4B). Since the activities of MKL1 and MKL2 are inhibited by monomeric actin [33], we next treated adipocytes with the actin depolymerizing agent Latrunculin B (LatB, 10 μ M). LatB disrupted actin filaments as shown using phalloidin staining and confocal microscopy (Fig 4C), providing a positive

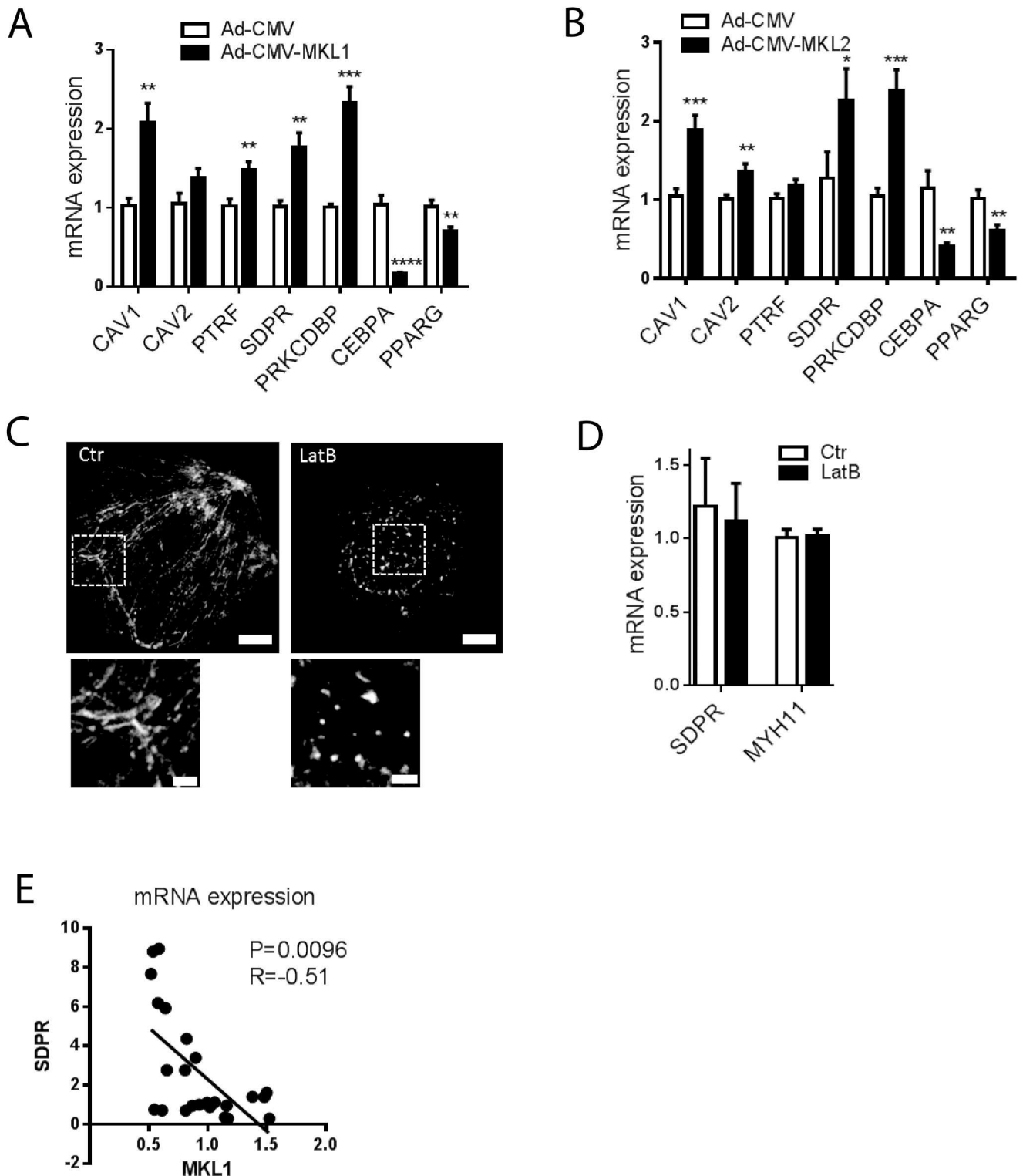


Fig 4. MKL1 and MKL2 drive expression of caveolins and cavins but SDPR expression is unresponsive to actin depolymerization in primary adipocytes. Panels **A** and **B** show expression of CAV1, CAV2, PTRF, SDPR and PRKCDBP in primary adipocytes following incubation with adenovirus encoding MKL1 (Ad-CMV-MKL1, **A**), MKL2 (Ad-CMV-MKL2, **B**) or control adenovirus (Ad-CMV-null). $n = 6-10$ independent experiments. Panel **C** shows actin staining in control adipocytes (Ctr, DMSO) and in adipocytes treated with latrunculin B (LatB) for 16h. Bars represent 10 μm in upper panels. Magnifications of actin cables, and puncta, respectively, are shown in the lower panels where bars represent 2 μm. $n = 3$ independent experiments where 10–15 images were captured per experiment. Panel **D** shows the SDPR mRNA level in

primary adipocytes following incubation in the absence and presence of LatB (10 μ M) for 16 h. Control cells (ctr) were incubated with DMSO. $n = 3$ independent experiments. Panel E shows that the mRNA levels for MKL1 and SDPR are negatively correlated during adipocyte differentiation. Data in panels A through D is presented as means \pm SEM, * $p \leq 0.05$, ** $p \leq 0.01$, *** $p \leq 0.001$ and **** $p \leq 0.0001$.

doi:10.1371/journal.pone.0173412.g004

control for the treatment effect, but had no effect on SDPR mRNA expression (Fig 4D). The prototypical MKL1 target MYH11 was similarly unresponsive (Fig 4D). This is very different from smooth muscle cells where LatB reduces SDPR by $\approx 70\%$ [21], arguing that SDPR expression is independent of actin polymerization, and thus presumably MKL1/MKL2 activity, in adipocytes.

Our experiments in adipocytes suggested the possibility that the transcriptional drive for SDPR may be shifted from MKLs towards PPAR γ /CEBP α during adipogenesis. If this was the case, one might expect a negative correlation between MKL1 and SDPR during differentiation. This was indeed seen (Fig 4E), further supporting the notion that MKL1 and PPAR γ /CEBP α are mutually antagonistic in the context of adipogenesis.

Discussion

This is, to the best of our knowledge, the first report demonstrating that two regulators of adipocyte differentiation, CEBP α and PPAR γ , regulate cavin-2 (SDPR) expression. Our current experiments constitute an important advancement of knowledge, showing significant induction of both cavin-1 (PTRF) and of cavin-2 (SDPR) following PPAR γ activation. In addition, findings in the present work demonstrate that in primary adipocytes, CEBP α can control cavin-2 (SDPR) expression independently of PPAR γ activity. Regulation of cavin-2 by CEBP α /PPAR γ may be considered an explanation for the high expression of cavin-2 in adipose tissue ([16, 19], present study) and potentially also in endothelial cells, where PPAR γ exerts important effects [34]. Loss of cavin-2 has been demonstrated to cause loss of caveolae in some tissues [15, 18, 19], supporting the view that it is an important organelle constituent. Our findings are therefore likely of direct relevance for biogenesis of caveolae.

Prior work has established that PPAR γ may drive expression of CAV1 and CAV2 [35, 36]. One of those studies found that adenoviral transduction of PPAR γ *in vivo* caused adipogenic transdifferentiation of hepatic cells together with a 30-fold induction of CAV1 [36]. The effect on CAV1 appears to be cell type-dependent, however, and in some cancer cell lines no effect of PPAR γ activation on CAV1 was observed [35]. The basis of this variability remains unexplored and the finding that PPAR γ regulates CAV1 predates the discovery of the cavins [37]. Here, we were unable to demonstrate an effect of PPAR γ activation on the CAV1 mRNA level in primary adipocytes and 3T3-L1 cells during differentiation. A well-established paradigm in the caveolae field is that formation of caveolae provides a scaffold that protects caveolins and cavins from degradation. It is possible that the effect of PPAR γ and CEBP α on cavin-2 may indirectly stabilize other caveolae constituents. This is also expected to provide an indirect way to regulate the density of caveolae at the cell membrane.

Beyond the novel finding that cavin-2/SDPR is controlled by CEBP α /PPAR γ in adipocytes, our results also confirm and extend the recent demonstration that myocardin family coactivators control the expression of caveolins and cavins [21]. In our previous study [21] we found that myocardin and MKL1 control gene expression of caveolins and cavins in smooth muscle. Herein, we demonstrate that MKL2, similar to MKL1, has the ability to drive transcription of all caveolins and cavins except cavin-1 (PTRF), in terminally differentiated, primary adipocytes. Several lines of evidence however argue against the idea that MKL1 and/or MKL2 provide a transcriptional drive for SDPR in normal, healthy adipocytes. First, MKL1 and MKL2 have been demonstrated to be markedly reduced during adipogenesis [22], a process in which

all caveolins and cavins increase. Here, we expand on the concept of a mutual antagonism between adipogenic and myogenic transcriptional influences by showing remarkable repression of both CEBP α and PPAR γ following MKL transduction. Second, we demonstrate that depolymerization of actin using Latrunculin B, which inhibits MKL activity and represses cavin-2/SDPR by 70% in smooth muscle [21], is without effect on cavin-2/SDPR (and caveolin-1) in primary rat adipocytes. Because Latrunculin B had an effect on actin polymerization in adipocytes, and in view of our finding that MKL mRNA was detectable, our results suggest that the MKLs may be transcriptionally silent in adipocytes, perhaps due to a high G- to F-actin ratio. An exciting possibility is that this would allow MKLs to assume a role under pathological conditions, such as in adipocyte hypertrophy, often linked to obesity and insulin resistance.

At least two observations in the present study merit special consideration because they are seemingly contradictory. The first is our finding that correlations between CEBP α and SDPR in human tissues are less consistent than are correlations between PPAR γ and SDPR, despite apparently larger effects of CEBP α than of PPAR γ overexpression *in vitro*. We can only speculate on the basis of this discrepancy. One potential explanation is that PPAR γ overexpression was made in mature adipocytes where the expression is already very high. PPAR γ was thus potentially present at saturating concentrations, and could only be further activated via a ligand. Alternatively, the smaller effect on SDPR was caused by the relatively smaller degree of overexpression (S1 Fig, panel A). With regard to the poor correlation between CEBP α and SDPR at the tissue level, we speculate that presence of other cell types may represent a confounding factor, but other CEBP isoforms, including CEBPG, could also play a role. Another perplexing finding was that rosiglitazone failed to directly activate an SDPR promoter reporter, despite considerable effectiveness in the context of intact chromatin. One explanation could be that the promoter reporter encompassed only 1263 nucleotides upstream of the transcription start site and thus potentially did not include the relevant regulatory element(s). ChIP-Seq peaks at SDPR locus (UCSC Genome Browser) seem to support the presence of a distal enhancer, but we do not rule out other explanations. Indeed, PPAR γ seems to be acting indirectly via induction of the CEBP α protein. This was suggested by the lack of additive effects of CEBP α overexpression and PPAR γ activation, and the fact that the latter induced the CEBP α protein in two different adipocyte models. Knock down of CEBP α moreover partly mitigated the effect of Rosiglitazone on SDPR. Some effect of Rosiglitazone remained under these conditions, but this is to be expected given that CEBP α was only partly reduced (by 60%).

To summarize, novel findings in this study include the demonstration that PPAR γ activation and CEBP α overexpression strongly regulate SDPR expression in adipocytes and that depolymerization of actin is without effects on SDPR expression in adipocytes, despite a capacity of MKL1 and MKL2 to increase mRNA levels of essentially all caveolins and cavins. This study, in conjunction with our previous work [21], thus highlights a considerable divergence between different cells types with regard to transcriptional control mechanisms of caveolar constituents. Such diversity may allow for tissue-specific pharmacological manipulation of caveolar function in diabetes and obesity.

Supporting information

S1 Fig. Efficiency of overexpression and MKL translocation. Panel A shows mRNA expression of CEBPA, MKL2 and PPARG in cells transduced with the respective virus. Panel B shows representative immunofluorescence images of a primary adipocyte expressing eGFP-MKL1 (nucleus in blue, left panel; eGFP signal in green, right panel), ScFigale bar = 10 μ m. (PDF)

Acknowledgments

We would like to thank Sam Cushman for scientific discussions and Dmitry Kamaev for downloading and TMM normalizing GTEx expression data.

Author Contributions

Conceptualization: BH CR DK SW JS OG K. Stenkula K. Swärd.

Formal analysis: BH CR DK OG K. Stenkula K. Swärd.

Funding acquisition: K. Stenkula K. Swärd.

Investigation: BH CR DK SW OG.

Methodology: BH CR OG K. Stenkula K. Swärd.

Project administration: K. Stenkula K. Swärd.

Resources: OG K. Stenkula K. Swärd.

Supervision: K. Stenkula K. Swärd.

Validation: BH CR OG K. Stenkula K. Swärd.

Writing – original draft: K. Stenkula K. Swärd.

Writing – review & editing: BH CR OG K. Stenkula K. Swärd.

References

1. Bastiani M, Parton RG. Caveolae at a glance. *Journal of cell science*. 2010; 123(Pt 22):3831–6. doi: [10.1242/jcs.070102](https://doi.org/10.1242/jcs.070102) PMID: [21048159](https://pubmed.ncbi.nlm.nih.gov/21048159/)
2. Stralfors P. Caveolins and caveolae, roles in insulin signalling and diabetes. *Advances in experimental medicine and biology*. 2012; 729:111–26. doi: [10.1007/978-1-4614-1222-9_8](https://doi.org/10.1007/978-1-4614-1222-9_8) PMID: [22411317](https://pubmed.ncbi.nlm.nih.gov/22411317/)
3. Cohen AW, Hnasko R, Schubert W, Lisanti MP. Role of caveolae and caveolins in health and disease. *Physiological reviews*. 2004; 84(4):1341–79. doi: [10.1152/physrev.00046.2003](https://doi.org/10.1152/physrev.00046.2003) PMID: [15383654](https://pubmed.ncbi.nlm.nih.gov/15383654/)
4. Nassar ZD, Parat MO. Cavin Family: New Players in the Biology of Caveolae. *Int Rev Cell Mol Biol*. 2015; 320:235–305. doi: [10.1016/bs.ircmb.2015.07.009](https://doi.org/10.1016/bs.ircmb.2015.07.009) PMID: [26614875](https://pubmed.ncbi.nlm.nih.gov/26614875/)
5. Kovtun O, Tillu VA, Ariotti N, Parton RG, Collins BM. Cavin family proteins and the assembly of caveolae. *Journal of cell science*. 2015; 128(7):1269–78. PubMed Central PMCID: [PMCPMC4379724](https://pubmed.ncbi.nlm.nih.gov/PMCPMC4379724/). doi: [10.1242/jcs.167866](https://doi.org/10.1242/jcs.167866) PMID: [25829513](https://pubmed.ncbi.nlm.nih.gov/25829513/)
6. Hayashi YK, Matsuda C, Ogawa M, Goto K, Tominaga K, Mitsuhashi S, et al. Human PTRF mutations cause secondary deficiency of caveolins resulting in muscular dystrophy with generalized lipodystrophy. *The Journal of clinical investigation*. 2009; 119(9):2623–33. PubMed Central PMCID: [PMCPMC2735915](https://pubmed.ncbi.nlm.nih.gov/PMCPMC2735915/). doi: [10.1172/JCI38660](https://doi.org/10.1172/JCI38660) PMID: [19726876](https://pubmed.ncbi.nlm.nih.gov/19726876/)
7. Kim CA, Delepine M, Boutet E, El Mourabit H, Le Lay S, Meier M, et al. Association of a homozygous nonsense caveolin-1 mutation with Berardinelli-Seip congenital lipodystrophy. *The Journal of clinical endocrinology and metabolism*. 2008; 93(4):1129–34. doi: [10.1210/jc.2007-1328](https://doi.org/10.1210/jc.2007-1328) PMID: [18211975](https://pubmed.ncbi.nlm.nih.gov/18211975/)
8. Minetti C, Sotgia F, Bruno C, Scartezzini P, Broda P, Bado M, et al. Mutations in the caveolin-3 gene cause autosomal dominant limb-girdle muscular dystrophy. *Nature genetics*. 1998; 18(4):365–8. doi: [10.1038/ng0498-365](https://doi.org/10.1038/ng0498-365) PMID: [9537420](https://pubmed.ncbi.nlm.nih.gov/9537420/)
9. Oshikawa J, Otsu K, Toya Y, Tsunematsu T, Hankins R, Kawabe J, et al. Insulin resistance in skeletal muscles of caveolin-3-null mice. *Proceedings of the National Academy of Sciences of the United States of America*. 2004; 101(34):12670–5. PubMed Central PMCID: [PMCPMC515114](https://pubmed.ncbi.nlm.nih.gov/PMCPMC515114/). doi: [10.1073/pnas.0402053101](https://doi.org/10.1073/pnas.0402053101) PMID: [15314230](https://pubmed.ncbi.nlm.nih.gov/15314230/)
10. Talukder MA, Preda M, Ryzhova L, Prudovsky I, Pinz IM. Heterozygous caveolin-3 mice show increased susceptibility to palmitate-induced insulin resistance. *Physiol Rep*. 2016; 4(6). PubMed Central PMCID: [PMCPMC4814890](https://pubmed.ncbi.nlm.nih.gov/PMCPMC4814890/).

11. Cohen AW, Razani B, Wang XB, Combs TP, Williams TM, Scherer PE, et al. Caveolin-1-deficient mice show insulin resistance and defective insulin receptor protein expression in adipose tissue. *Am J Physiol Cell Physiol*. 2003; 285(1):C222–35. doi: [10.1152/ajpcell.00006.2003](https://doi.org/10.1152/ajpcell.00006.2003) PMID: [12660144](https://pubmed.ncbi.nlm.nih.gov/12660144/)
12. Karlsson M, Thorn H, Danielsson A, Stenkula KG, Ost A, Gustavsson J, et al. Colocalization of insulin receptor and insulin receptor substrate-1 to caveolae in primary human adipocytes. Cholesterol depletion blocks insulin signalling for metabolic and mitogenic control. *European journal of biochemistry / FEBS*. 2004; 271(12):2471–9. Epub 2004/06/09.
13. Gustincich S, Vatta P, Goruppi S, Wolf M, Saccone S, Della Valle G, et al. The human serum deprivation response gene (SDPR) maps to 2q32-q33 and codes for a phosphatidylserine-binding protein. *Genomics*. 1999; 57(1):120–9. doi: [10.1006/geno.1998.5733](https://doi.org/10.1006/geno.1998.5733) PMID: [10191091](https://pubmed.ncbi.nlm.nih.gov/10191091/)
14. Mineo C, Ying YS, Chapline C, Jaken S, Anderson RG. Targeting of protein kinase Calpha to caveolae. *The Journal of cell biology*. 1998; 141(3):601–10. PubMed Central PMCID: [PMC2132740](https://pubmed.ncbi.nlm.nih.gov/PMCID/PMC2132740/). PMID: [9566962](https://pubmed.ncbi.nlm.nih.gov/9566962/)
15. Hansen CG, Bright NA, Howard G, Nichols BJ. SDPR induces membrane curvature and functions in the formation of caveolae. *Nature cell biology*. 2009; 11(7):807–14. PubMed Central PMCID: [PMC2712677](https://pubmed.ncbi.nlm.nih.gov/PMCID/PMC2712677/). doi: [10.1038/ncb1887](https://doi.org/10.1038/ncb1887) PMID: [19525939](https://pubmed.ncbi.nlm.nih.gov/19525939/)
16. Bastiani M, Liu L, Hill MM, Jedrychowski MP, Nixon SJ, Lo HP, et al. MURC/Cavin-4 and cavin family members form tissue-specific caveolar complexes. *The Journal of cell biology*. 2009; 185(7):1259–73. PubMed Central PMCID: [PMC2712963](https://pubmed.ncbi.nlm.nih.gov/PMCID/PMC2712963/). doi: [10.1083/jcb.200903053](https://doi.org/10.1083/jcb.200903053) PMID: [19546242](https://pubmed.ncbi.nlm.nih.gov/19546242/)
17. Aboulaich N, Vainonen JP, Stralfors P, Vener AV. Vectorial proteomics reveal targeting, phosphorylation and specific fragmentation of polymerase I and transcript release factor (PTRF) at the surface of caveolae in human adipocytes. *The Biochemical journal*. 2004; 383(Pt 2):237–48. PubMed Central PMCID: [PMC1134064](https://pubmed.ncbi.nlm.nih.gov/PMCID/PMC1134064/). doi: [10.1042/BJ20040647](https://doi.org/10.1042/BJ20040647) PMID: [15242332](https://pubmed.ncbi.nlm.nih.gov/15242332/)
18. Breen MR, Camps M, Carvalho-Simoes F, Zorzano A, Pilch PF. Cholesterol depletion in adipocytes causes caveolae collapse concomitant with proteosomal degradation of cavin-2 in a switch-like fashion. *PloS one*. 2012; 7(4):e34516. PubMed Central PMCID: [PMC3321009](https://pubmed.ncbi.nlm.nih.gov/PMCID/PMC3321009/). doi: [10.1371/journal.pone.0034516](https://doi.org/10.1371/journal.pone.0034516) PMID: [22493697](https://pubmed.ncbi.nlm.nih.gov/22493697/)
19. Hansen CG, Shvets E, Howard G, Riento K, Nichols BJ. Deletion of cavin genes reveals tissue-specific mechanisms for morphogenesis of endothelial caveolae. *Nature communications*. 2013; 4:1831. PubMed Central PMCID: [PMC3674239](https://pubmed.ncbi.nlm.nih.gov/PMCID/PMC3674239/). doi: [10.1038/ncomms2808](https://doi.org/10.1038/ncomms2808) PMID: [23652019](https://pubmed.ncbi.nlm.nih.gov/23652019/)
20. Regazzetti C, Dumas K, Lacas-Gervais S, Pastor F, Peraldi P, Bonnafous S, et al. Hypoxia inhibits Cavin-1 and Cavin-2 expression and down-regulates caveolae in adipocytes. *Endocrinology*. 2015; 156(3):789–801. doi: [10.1210/en.2014-1656](https://doi.org/10.1210/en.2014-1656) PMID: [25521582](https://pubmed.ncbi.nlm.nih.gov/25521582/)
21. Krawczyk KK, Yao Mattisson I, Ekman M, Oskolkov N, Granting R, Kotowska D, et al. Myocardin Family Members Drive Formation of Caveolae. *PloS one*. 2015; 10(8):e0133931. PubMed Central PMCID: [PMC4526231](https://pubmed.ncbi.nlm.nih.gov/PMCID/PMC4526231/). doi: [10.1371/journal.pone.0133931](https://doi.org/10.1371/journal.pone.0133931) PMID: [26244347](https://pubmed.ncbi.nlm.nih.gov/26244347/)
22. McDonald ME, Li C, Bian H, Smith BD, Layne MD, Farmer SR. Myocardin-related transcription factor A regulates conversion of progenitors to beige adipocytes. *Cell*. 2015; 160(1–2):105–18. PubMed Central PMCID: [PMC4384505](https://pubmed.ncbi.nlm.nih.gov/PMCID/PMC4384505/). doi: [10.1016/j.cell.2014.12.005](https://doi.org/10.1016/j.cell.2014.12.005) PMID: [25579684](https://pubmed.ncbi.nlm.nih.gov/25579684/)
23. Nobusue H, Onishi N, Shimizu T, Sugihara E, Oki Y, Sumikawa Y, et al. Regulation of MKL1 via actin cytoskeleton dynamics drives adipocyte differentiation. *Nature communications*. 2014; 5:3368. doi: [10.1038/ncomms4368](https://doi.org/10.1038/ncomms4368) PMID: [24569594](https://pubmed.ncbi.nlm.nih.gov/24569594/)
24. Tontonoz P, Hu E, Spiegelman BM. Stimulation of adipogenesis in fibroblasts by PPAR gamma 2, a lipid-activated transcription factor. *Cell*. 1994; 79(7):1147–56. PMID: [8001151](https://pubmed.ncbi.nlm.nih.gov/8001151/)
25. Rosen ED, Spiegelman BM. Molecular regulation of adipogenesis. *Annu Rev Cell Dev Biol*. 2000; 16:145–71. doi: [10.1146/annurev.cellbio.16.1.145](https://doi.org/10.1146/annurev.cellbio.16.1.145) PMID: [11031233](https://pubmed.ncbi.nlm.nih.gov/11031233/)
26. Haakonsson AK, Stahl Madsen M, Nielsen R, Sandelin A, Mandrup S. Acute genome-wide effects of rosiglitazone on PPARgamma transcriptional networks in adipocytes. *Mol Endocrinol*. 2013; 27(9):1536–49. doi: [10.1210/me.2013-1080](https://doi.org/10.1210/me.2013-1080) PMID: [23885096](https://pubmed.ncbi.nlm.nih.gov/23885096/)
27. Rodbell M. Metabolism of Isolated Fat Cells. I. Effects of Hormones on Glucose Metabolism and Lipolysis. *The Journal of biological chemistry*. 1964; 239:375–80. Epub 1964/02/01. PMID: [14169133](https://pubmed.ncbi.nlm.nih.gov/14169133/)
28. Livak KJ, Schmittgen TD. Analysis of relative gene expression data using real-time quantitative PCR and the 2(-Delta Delta C(T)) Method. *Methods*. 2001; 25(4):402–8. doi: [10.1006/meth.2001.1262](https://doi.org/10.1006/meth.2001.1262) PMID: [11846609](https://pubmed.ncbi.nlm.nih.gov/11846609/)
29. Stenkula KG, Lizunov VA, Cushman SW, Zimmerberg J. Insulin controls the spatial distribution of GLUT4 on the cell surface through regulation of its postfusion dispersal. *Cell metabolism*. 2010; 12(3):250–9. Epub 2010/09/08. PubMed Central PMCID: [PMC3427691](https://pubmed.ncbi.nlm.nih.gov/PMCID/PMC3427691/). doi: [10.1016/j.cmet.2010.08.005](https://doi.org/10.1016/j.cmet.2010.08.005) PMID: [20816091](https://pubmed.ncbi.nlm.nih.gov/20816091/)

30. Lindahl M, Petrlova J, Dalla-Riva J, Wasserstrom S, Rippe C, Domingo-Espin J, et al. ApoA-I Milano stimulates lipolysis in adipose cells independently of cAMP/PKA activation. *Journal of lipid research*. 2015; 56(12):2248–59. PubMed Central PMCID: PMC4655981. doi: [10.1194/jlr.M054767](https://doi.org/10.1194/jlr.M054767) PMID: [26504176](https://pubmed.ncbi.nlm.nih.gov/26504176/)
31. Henriksson E, Sall J, Gormand A, Wasserstrom S, Morrice NA, Fritzen AM, et al. SIK2 regulates CRTCs, HDAC4 and glucose uptake in adipocytes. *Journal of cell science*. 2015; 128(3):472–86. PubMed Central PMCID: PMC4311129. doi: [10.1242/jcs.153932](https://doi.org/10.1242/jcs.153932) PMID: [25472719](https://pubmed.ncbi.nlm.nih.gov/25472719/)
32. Consortium GT. The Genotype-Tissue Expression (GTEx) project. *Nature genetics*. 2013; 45(6):580–5. PubMed Central PMCID: PMC4010069. doi: [10.1038/ng.2653](https://doi.org/10.1038/ng.2653) PMID: [23715323](https://pubmed.ncbi.nlm.nih.gov/23715323/)
33. Olson EN, Nordheim A. Linking actin dynamics and gene transcription to drive cellular motile functions. *Nature reviews Molecular cell biology*. 2010; 11(5):353–65. PubMed Central PMCID: PMC3073350. doi: [10.1038/nrm2890](https://doi.org/10.1038/nrm2890) PMID: [20414257](https://pubmed.ncbi.nlm.nih.gov/20414257/)
34. Panigrahy D, Singer S, Shen LQ, Butterfield CE, Freedman DA, Chen EJ, et al. PPARgamma ligands inhibit primary tumor growth and metastasis by inhibiting angiogenesis. *The Journal of clinical investigation*. 2002; 110(7):923–32. PubMed Central PMCID: PMC151148. doi: [10.1172/JCI15634](https://doi.org/10.1172/JCI15634) PMID: [12370270](https://pubmed.ncbi.nlm.nih.gov/12370270/)
35. Burgermeister E, Tencer L, Liscovitch M. Peroxisome proliferator-activated receptor-gamma upregulates caveolin-1 and caveolin-2 expression in human carcinoma cells. *Oncogene*. 2003; 22(25):3888–900. doi: [10.1038/sj.onc.1206625](https://doi.org/10.1038/sj.onc.1206625) PMID: [12813462](https://pubmed.ncbi.nlm.nih.gov/12813462/)
36. Gavrilova O, Haluzik M, Matsusue K, Cutson JJ, Johnson L, Dietz KR, et al. Liver peroxisome proliferator-activated receptor gamma contributes to hepatic steatosis, triglyceride clearance, and regulation of body fat mass. *The Journal of biological chemistry*. 2003; 278(36):34268–76. Epub 2003/06/14. doi: [10.1074/jbc.M300043200](https://doi.org/10.1074/jbc.M300043200) PMID: [12805374](https://pubmed.ncbi.nlm.nih.gov/12805374/)
37. Hill MM, Bastiani M, Luetterforst R, Kirkham M, Kirkham A, Nixon SJ, et al. PTRF-Cavin, a conserved cytoplasmic protein required for caveola formation and function. *Cell*. 2008; 132(1):113–24. PubMed Central PMCID: PMC2265257. doi: [10.1016/j.cell.2007.11.042](https://doi.org/10.1016/j.cell.2007.11.042) PMID: [18191225](https://pubmed.ncbi.nlm.nih.gov/18191225/)